Landau theory of structures in tetragonal-orthorhombic ferroelastics

A. E. Jacobs*

Department of Physics, University of Toronto, Toronto, Ontario, Canada M5S 1A7
and Department of Physics of Complex Systems, Weizmann Institute of Science, Rehovot, Israel 76100
(Received 24 September 1999)

A Landau expansion of the elastic energy in the strains is used to study two-dimensional structures in tetragonal-orthorhombic ferroelastics with constraints. Local energy minima are found with respect to the components of the displacement and so the strains satisfy the compatibility relation; this interdependence of the strains, combined with the constraints, can give rise to a subtle frustration. Extraordinarily, a complex energy surface with many bulk metastable states results purely from boundary conditions, without bulk inhomogeneities (such as impurities) of any sort. Some settings require twin walls in only one set of tetragonal 110-type planes; only two variants appear, and the dilatational and shear strains are localized near the surface. Tip splitting can occur when twin walls collide with fixed boundaries. Other settings require both 110 and 1$\bar{1}$0 walls and so all four variants appear. The structures resulting from collisions of the two twin families are so complex that the ground state of a large system cannot be found with confidence. Strange walls appear between variants with identical deviatoric strain. The dilatational and shear strains are large also in the bulk. Walls wobble, bow, and bend counterintuitively, and pairs sometimes pinch in. Study of the rotation is shown to be essential for understanding some aspects of the structures, particularly collisions of orthogonal twin bands. The ferroelastic-ferromagnet analogy is found to be misleading in important respects. Tip splitting, pinching-in, wall wobbling, and other phenomena are seen in electron microscopy of YBa$_2$Cu$_3$O$_{7-\delta}$ and other materials.

I. INTRODUCTION

Ferroelastic transformations are diffusionless, first-order, shape-changing, phase changes in the solid state.[1,2] In cubic-tetragonal (C-T) systems (like Nb$_3$Sn, V$_3$Si, In-Tl, and Fe-Pd alloys), for example, the cubic unit cell elongates (or contracts) along one of three axes to form a tetragonal unit cell; below the transition temperature T_c there are three possible homogeneous products (variants) differing only in orientation. The name ferroelastic is best reserved for materials in which the strain energy dominates the morphology and the kinetics, giving elastic hysteresis, defects stable on laboratory time scales, slow relaxation, glassy behavior, the ''tweed'' structure, the shape-memory effect, and like phenomena. One speaks of ferroelastic transformations, not transitions (on cooling, the product often first appears at a temperature much higher than that where the parent disappears).

Although the walls cost energy, ferroelastics below T_c almost always contain multiple variants, likely most often due to constraints. For example, grains in a polycrystalline material prevent their neighbors from distorting by more than a few times 10^{-11} m, much less than required by a typical strain of 10^{-4} in a grain of typical width 10^{-4} m, and so a homogeneous product would require huge stresses. The multiple goals of (a) gaining the transformation energy, (b) maintaining the external shape, and (c) relieving the stresses are achieved by transformation to an inhomogeneous product. Most of the sample transforms fully, but a portion forms walls separating the variants; the displacements from the different variants alternate in sign, much reducing the displacement at the surface and thereby relieving the stresses. Multiple variants may result also from separate nucleation events, or from the growth of the nucleus; or they may be relics of the nucleation process itself. Whatever their

origin, they reduce the shape change otherwise generated by a uniform distortion, just as domains in ferromagnets reduce the field energy otherwise generated by a uniform magnetization. Though responsible for the very name ferroelastic,[1] the analogy with ferromagnets is however often taken far too seriously, as seen below.

The theory of the morphology of ferromagnets is mature both analytically and numerically, say to find the domain structure that minimizes the global energy. The theory of ferroelastics deals with the analogous ''accommodation problem,'' the puzzle of how to assemble variants so as to minimize the energy, in the presence of constraints; this theory is in its infancy. The analogy is formally correct at the Landau-theory level, but it fails at the next step, a point not always appreciated. The magnetic energy is expanded in the magnetization **m** (and derivatives), and must be minimized with respect to **m**. The elastic energy is expanded in the strains e_k (and derivatives), but must *not* be minimized with respect to the e_k in inhomogeneous situations, because the second derivatives of the e_k are not independent. The result is a subtle frustration absent from the theory of ferromagnets.

The ''nucleation problem'' in ferroelastics is a mystery. Classical (droplet) nucleation theory fails completely, another failure of the analogy; because the transition is first order, the product-parent interface generates prohibitively large dilatational and shear energies, whether the nucleation is heterogeneous or homogeneous. The nucleus must instead contain several products (perhaps incompletely developed) arranged in some manner (perhaps twinned) to give small displacement at the interface. Studies of constrained systems, like those reported below, may then advance our understanding of ferroelastic nucleation.

When the strain is the primary order parameter, the Landau theory is a relatively simple expansion in the strains and

their derivatives. But in most cases the strain is induced, as in $YBa_2Cu_3O_{7-\delta}$ where the tetragonal-orthorhombic (T-O) transition results from oxygen ordering in the chains. If the strain energy dominates, however, a theory including only strain terms (with appropriate coefficients, perhaps T dependent) should describe adequately the ferroelastic properties. Or it may be possible to eliminate the primary order parameter and get a strain-only energy.[3]

The first application[4] of Landau theory to inhomogeneous ferroelastics treated the one-dimensional (1D) problem, with a scalar displacement and one strain. The discovery[5] of an analytical solution for the product-product soliton of the C-T transformation was a pivotal contribution, not so much because of the correct prediction that the wall is parallel to cubic 110-type planes (much was known then about domain-wall orientations in ferroelastics[6]), but rather because it showed how the power and insight of Landau theory can be brought to bear on inhomogeneous ferroelastics. Although the solution applies at only one temperature, and although no C-T analytical solution exists at any other T, Ref. 5 opened the way for understanding many aspects of ferroelastics.

But the 1D problem lacks essential physics, and the 3D problem requires massive computational resources for further progress. The 2D T-O problem[7] has the right stuff for understanding the morphology, namely the hidden frustration (lacking in $1D$) from the interdependence of the strains, and it has been used in most advances since Ref. 5. It has direct application to important physical systems like $YBa_2Cu_3O_{7-\delta}$. It allows analytical solutions[7,8] for the product-product wall at all T, and the parent-product wall at $T=T_c$. It allows numerical studies[9–11] which have explained various phenomena including the tweed structure observed by a variety of techniques in a host of materials,[9,10] the entry of twin walls to relieve stresses due to boundary conditions,[11] and why ferroelastic transformations are typically spread over a temperature interval.[11] It allows fascinating studies[12,13] of the dynamics, especially the formation and growth of a twinned square-rectangular nucleus. Finally, it is a preliminary to understanding C-T ferroelastics, though C-T numerical studies will likely provide major surprises.

Of course other approaches[14,15] have been used to study the statics and dynamics of ferroelastics, including the tweed structure, as described in Ref. 10; see also Ref. 16.

This paper continues the Landau-theory study of static structures in T-O ferroelastics. Section II sets up the expression for the elastic energy, and Sec. III presents results obtained by numerical minimization of the energy for several physical settings.

(1) For square-columnar grains with fixed boundaries parallel to T 100-type planes, the ground state contains a set of twin walls parallel to T 110-type planes (which are optimal); only two of the four variants appear and the dilatational and shear strains are large only near the boundaries. Structures with higher energy (and with walls of both 110 types) are found, however, and are more common in larger systems.

(2) For square-columnar grains with fixed boundaries parallel to 110-type planes, both 110 and $1\bar{1}0$ twin families are required, giving collisions between them; the dilatational and shear strains are large at the 90° wall bends, and all four variants appear. The walls often deviate from 110-type planes, and they bow and wobble strangely near walls of the other family. Many metastable structures are found, so many that the ground state of a large system cannot be found with confidence.

(3) When a twin band collides at 90° with an obstacle (such as a grain boundary or walls of the other twin family), alternate pairs of twin walls in the first band pinch in at a strange wall between two variants with identical deviatoric strain. The same phenomenon is seen also for 110-type grains. A Landau-level understanding of the pinching-in requires study of the rotation, done in Sec. III for the first time.

(4) When pairs of twin walls retract through an orthogonal wall (and obviously in the reverse process), narrow tips become broad and *vice versa*.

(5) Tip splitting can occur when twin walls collide with a grain boundary at 45°.

(6) The transformation front between T parent and twinned O product (in, for example, a temperature gradient) is parallel to 100-type planes, as in Ref. 12; that is, the front does not zigzag by forming T-O walls.

The 90° bends, the pinching-in, the bowing and wobbling, and the tip splitting (the last with differences) are observed in $Pb_3(PO_4)_2$ and $YBa_2Cu_3O_{7-\delta}$ for example, as in Figs. 7.9, 7.16, and 7.17 of Ref. 2 and Figs. 2 of Refs. 17 and 18. These effects (save perhaps the 90° bends) have no parallel in anisotropic ferromagnets, another failure of the analogy.

The complexity of the energy surface is remarkable,[19] for it is a bulk effect whose sole cause is a bounding surface, without impurities or bulk inhomogeneities of any kind. Of course it has long been known that strains have long-range effects, but this seems nevertheless an extraordinary result. It is not known how the number of metastable states scales with the size of the system; neither is anything known theoretically about the dynamics of constrained systems. The issue, which seems important for the interpretation of experiments and also in principle, is whether glassy behavior is intrinsic to constrained ferroelastics or whether it requires inhomogeneities like impurities. Simulations might answer the interesting question: can a surface alone produce glassy behavior in the bulk?

II. ELASTIC ENERGY

The high-T (parent) state is tetragonal, and the low-T (product) state orthorhombic. The 3 axis of the body coordinate system lies along the fourfold axis of the T state; the 1 and 2 axes are twofold axes, and the 1-3 and 2-3 planes are mirror planes. The displacement field is $\mathbf{u} = \mathbf{x'} - \mathbf{x}$ where $\mathbf{x}$ and $\mathbf{x'}$ are the coordinates of a material point in the undeformed and deformed states, respectively. Computational resources limit the study to structures uniform in the 3 direction (and so 90° twist grain boundaries are omitted); on the other hand, the 2D structures are those most easily studied experimentally. Then $\mathbf{u}$ lies in the 1-2 plane, it depends on only x_1 and x_2, and so three strains vanish identically.

The three remaining strains (all of which vanish in the T state) are obtained from the displacement $\mathbf{u}$ through the symmetric strain tensor η:

$$e_1 = (\eta_{11} + \eta_{22})/\sqrt{2}, \tag{2.1a}$$

$$e_2 = (\eta_{11} - \eta_{22})/\sqrt{2}, \tag{2.1b}$$

$$e_6 = \eta_{12}, \qquad (2.1c)$$

$$\eta_{ij} = \frac{1}{2}(u_{i,j} + u_{j,i} + u_{k,i}u_{k,j}), \qquad (2.2)$$

in the Lagrangian description.[20] Here $i,j,k=1$ or 2, $u_{i,j} = \partial_j u_i = \partial u_i / \partial x_j$, and repeated indices are summed. More reasonable definitions for e_1 and e_2 would have denominators 2, not $\sqrt{2}$. These are called the dilatational, deviatoric, and shear strains, respectively, though e_1 is simply related to the true dilatational strain e_0 only in the limit of infinitesimal strains; it is the strain e_2 which is nonzero below the transition. To understand some aspects of the structures, one must study also the fourth combination of the $u_{i,j}$, the rotation

$$\omega_3 = \frac{1}{2}(u_{1,2} - u_{2,1}); \qquad (2.3)$$

explicitly, for a uniform rotation by an angle ϕ about the 3 axis, $\omega_3 = \sin\phi$ and all $\eta_{ij} = 0$.

The elastic energy F is the integral of the density $\mathcal{F}$ over the undeformed space A:

$$F = \int_A \mathcal{F} \, dx_1 \, dx_2. \qquad (2.4)$$

Clearly $\mathcal{F}$ can depend on $\mathbf{u}$ and ω_3 only through their derivatives. To leading order, $\mathcal{F}$ is the sum $\mathcal{F} = \mathcal{F}_s\{e_i\} + \mathcal{F}_{sg}\{e_{i,j}\}$ of separate contributions from the strains and their derivatives.

For the strain terms in $\mathcal{F}$, the simplest expression consistent with the requirements is

$$\mathcal{F}_s\{e_i\} = \frac{1}{2}A_1 e_1^2 + \frac{1}{2}A_2 e_2^2 + \frac{1}{4}B_2 e_2^4 + \frac{1}{6}C_2 e_2^6 + \frac{1}{2}A_6 e_6^2$$
$$(2.5a)$$

relative to the T state.[7] At high T, the terms $\frac{1}{2}A_k e_k^2$ are the usual contributions for a linear, homogeneous, elastic medium, and the coefficients A_k are all positive; in Voigt notation,[20] $A_1 = C_{11} + C_{12}$, $A_2 = C_{11} - C_{12}$, and $A_6 = 4C_{44}$. In Landau theory, however, the coefficient A_2 depends on T as $A_2 = a(T - T_0)$ (with $a > 0$) and so the T state is unstable at low T; for a first-order transition, $B_2 < 0$ and the term in e_2^6 (with $C_2 > 0$) is needed for stability. The transition temperature T_c (which is $> T_0$) is found from[21] $A_2 = 3B_2^2/(16C_2)$. The homogeneous O state (with $e_1 = e_6 = 0$) is twofold degenerate; a square with sides parallel to the T 100 and T 010 axes deforms to a rectangle with long side parallel to the first ($e_2 = +e_{20}$) or the second ($e_2 = -e_{20}$), where $e_{20} = [(-\frac{1}{2}B_2 + \gamma)/C_2]^{1/2}$ and $\gamma = (\frac{1}{4}B_2^2 - A_2 C_2)^{1/2}$. The transformation energy is the energy of the homogeneous O state, with density $\mathcal{F}_O = \frac{1}{2}A_2 e_{20}^2 + \frac{1}{4}B_2 e_{20}^4 + \frac{1}{6}C_2 e_{20}^6$.

The strain-gradient part of $\mathcal{F}$ is (from Appendix A)

$$\mathcal{F}_{sg}\{e_{i,j}\} = \frac{1}{2}d_1(\vec{\nabla}e_1)^2 + \frac{1}{2}d_2(\vec{\nabla}e_2)^2 + \frac{1}{2}d_3(\vec{\nabla}e_6)^2. \qquad (2.5b)$$

The term $\frac{1}{2}d_2(\vec{\nabla}e_2)^2$ is crucial, for it gives walls a positive energy and sets their length scale [as in Eq. (2.7) below].

Without it, a constraint of zero overall displacement can be satisfied by microtwinning, an unphysical subdivision on arbitrarily fine scales.

The total density $\mathcal{F} = \mathcal{F}_s + \mathcal{F}_{sg}$ can then be written as the sum $\mathcal{F} = \mathcal{F}_1[e_1] + \mathcal{F}_2[e_2] + \mathcal{F}_6[e_6]$ of three uncoupled densities, each a functional (a polynomial plus a squared gradient) of a single strain. In homogeneous problems (all strain gradients $=0$), the energy is correctly minimized by $\delta F/\delta e_k = 0$, giving $e_2 = \pm e_{20}$, $e_1 = e_6 = 0$. In inhomogeneous problems, on the other hand, it is entirely wrong to minimize the energy with respect to the strains. The energy must instead be minimized with respect to the displacement ($\delta F/\delta u_i = 0$). Even when the densities are uncoupled, the strain gradients are coupled by the compatibility relations (necessary and sufficient conditions that the strains be derivable from the displacement). In two dimensions there is only one relation,

$$\eta_{11,22} + \eta_{22,11} - 2\eta_{12,12} = 0 \qquad (2.6a)$$

in terms of the strain tensor and

$$e_{1,11} + e_{1,22} - \sqrt{8}\, e_{6,12} - e_{2,11} + e_{2,22} = 0 \qquad (2.6b)$$

in terms of the strains, both for the linearized strain tensor.[22,23] The energy function of inhomogeneous ferroelastics then contains a subtle frustration (obviously absent in 1D) which is partially responsible for the complexity of the structures described below.

The energy must be minimized numerically in general (as in Ref. 11), but some analytical solutions exist.[7,8] Equation (2.6b) shows that solutions with $e_1 \equiv e_6 \equiv 0$ are possible if e_2 satisfies the wave equation, so that e_2 is a function of either $x_1 + x_2$ or $x_1 - x_2$ (but of course not a sum of the two); the reduction to a 1D problem for e_2 was discussed also in Refs. 5 and 7–11. The point is that the T 110 and $1\bar{1}0$ planes are optimal for walls; other orientations are possible, of course (they just cost more energy).

The O-O′ soliton (a twin wall) has a standard form for a first-order transition:

$$e_2(X) = e_{20}\sinh(X/\xi)/[\cosh^2(X/\xi) + \alpha]^{1/2}, \qquad (2.7)$$

where $X = (x_1 \pm x_2)/\sqrt{2}$, $\alpha = (-B_2 + 2\gamma)/(B_2 + 4\gamma)$, and $\xi = e_{20}^{-1}(d_2/\gamma)^{1/2}$ is the wall thickness parameter; ξ decreases with T, with $\xi \propto 1/\sqrt{A_2}$ at low T. This solution links the two variants, but it also rotates them by an angle ϕ, as shown in Refs. 5,7,8; from Eq. (A2) below, $\omega_3(X) = \pm e_2(X)/\sqrt{2}$ and so $\phi \approx e_{20}/\sqrt{2}$. In more detail, walls of the 110 family join variants with long sides at $-\phi$ and $\pi/2 + \phi$ to the T 100 axis, and walls of the $1\bar{1}0$ family join the other two. In twin walls then, $\omega_3 > 0$ in one variant, < 0 in the other, and $=0$ in the center (modulo a global rotation).

In the presence of both wall families, all four variants appear, creating two new kinds of wall. One separates variants with opposite e_2 and identical ω_3; the angle between the long axes is $\pi/2$ (rather than $\pi/2 - 2\phi$ as for twin walls). The other separates variants with identical e_2 and opposite ω_3; the angle between the long axes is 2ϕ. The analogy fails yet again; in ferromagnets, domain walls do not increase the

number of variants, and the strange 2ϕ wall has no counterpart. If the microscope is sensitive only to the deviatoric strain, then the first kind looks like a twin wall and the second is invisible. Both require dilatational and shear strains (unlike twin walls). If taken literally, they are high-energy configurations; in fact, their energy increases faster than linearly with the length. Section III finds that the necessary relaxation occurs by variant narrowing, combined with inhomogeneous rotation.

The Landau approach is expected to be especially good for ferroelastics (because of the long-range effect of strains), but it has weak points. First, Eq. (2.5) contains too many unmeasured parameters to attempt a quantitative description of a particular material, even though it omits many terms of the same order as those retained; only a qualitative description can be attempted. Second, the Landau theory is limited to $T \approx T_c$; for example, the homogeneous strain e_{20} does not saturate as A_2 decreases. A mean-field theory would be preferable at $T \ll T_c$, but this requires a specific model. Third, using gradients to represent the energy of inhomogeneous states implicitly assumes that the strains vary slowly over atomic distances; the high-resolution images of Ref. 2 (Fig. 8.6) and Refs. 17 and 18 show however that walls are only a few atomic separations wide. The counter to all three objections is that a qualitative understanding is what is required at present.

III. STRUCTURES

Appendix B gives the values of the Landau parameters and details of the numerics. The side length L of all figures is $L = 20$.

A. Square-columnar grain with 100-type boundaries

The displacement vanishes on and outside a square column with sides parallel to T 100-type planes, as in Ref. 11. The structures, which are up to 16-fold degenerate under symmetry operations, were found by quenches from random starting states.

Ten quenches for $L = 20$ (with grid size $h = 0.1$) gave four structures with energies ranging from 79% to 77% of the transformation energy; a few more structures may exist. Figure 1 gives a contour plot of the deviatoric strain for the ground state (found six times). The product-product walls are parallel to one set of T 110-type planes, though bent toward the corners. The strain is odd about one main diagonal; along a vertical (or horizontal) through the center of the square then, the net displacement is obviously zero to first order in e_2. The dilatational and shear strains (not shown) are large only near the boundaries, as in Ref. 11.

Ten quenches for larger grains ($L = 40$ with $h = 0.2$) all gave distinct structures. The lowest-energy structure, believed to be the ground state, contained a set of parallel walls (as in Fig. 1), but with some bowing.

B. Square-columnar grain with 110-type boundaries

The same introductory comments apply here, except that the sides are parallel to T 110-type planes. This setting requires both twin families and so collisions between them.

FIG. 1. Grayscale contour plot of the deviatoric strain e_2 for the ground state of a square-columnar grain with sides parallel to T 100-type planes. The black→white range is $-2.20 \times 10^{-3} \rightarrow +2.20 \times 10^{-3}$.

One hundred quenches for $L = 20$ (and $h = 0.1$) found 46 distinct structures; energies ranged from 82 to 78% of the transformation energy, with structures concentrated at the lower energies. Of the 46, 25 were found only once, with most of these at higher energies; likely many other solutions remain undiscovered even in this small system. Figure 2 shows the deviatoric strain for the lowest-energy state (found six times and believed to be the ground state); the walls form 90° bends and they bow away from the 110 and $1\bar{1}0$ planes. The domain configurations for this and the other 45 structures are quite unlike those in ferromagnets. Large dilatational and shear strains appear in the bulk as well as near the boundaries, especially near the bends; for the structure of Fig. 2, the maximum and minimum values are $\pm 3.17 \times 10^{-3}$ for e_1 and $\pm 2.05 \times 10^{-3}$ for e_6, both comparable to $e_{20} \approx 2.19 \times 10^{-3}$.

FIG. 2. Grayscale contour plot of the deviatoric strain e_2 for the ground state of a square-columnar grain with sides parallel to T 110-type planes. The black → white range is $-2.21 \times 10^{-3} \rightarrow +2.20 \times 10^{-3}$.

Thirty quenches for larger L ($L=40$ with $h=0.2$) all gave distinct structures, with patterns more complicated than in the smaller systems; the best (almost certainly not the ground state) had 89% of the transformation energy. There is no room for doubt here: the walls are bulk defects, and they are produced by the boundary conditions and the frustration.

A few quenches for smaller systems found multiple structures for L as small as 5.

C. Comments on structures in grain settings

The Landau theory explains qualitatively the counterintuitive wall bending, bowing, and wobbling seen in experiment. The theoretical energy surface is complex for both grain settings (though less so for 100-type grains) and it will clearly be complex whatever the shape of the grain. The observed patterns[2,17,18] suggest a complex energy surface, but they are far less contorted than found theoretically; they are dominated by large bands of parallel twin walls, suggesting heterogeneous nucleation, whereas the numerical procedure favors homogeneous nucleation. More ordered starting configurations for the model quenches might produce patterns more like those seen experimentally. Perhaps quick cooling to low T would favor homogeneous nucleation and produce structures more like those found theoretically. The appearance of different structures on repeated cooling would provide strong evidence for a complex energy surface; shape-memory materials seem unsuitable for this purpose, for in them the domain patterns are reproducible almost by definition.

D. Variant narrowing

The termination of one twin band by an orthogonal band is often observed;[2,17,18] strangely, alternate variants of the impinging band narrow and broaden (as seen in many structures of 110-type grains above). The following shows that an understanding of the effect requires study of the rotation (which is not immediately available in theories[14,15,12,13] which push the analogy with ferromagnets and deal largely or exclusively with the deviatoric strain).

Figure 3(a) shows schematically the unrelaxed configuration for a pair of twin walls colliding with an orthogonal band; in all parts of Fig. 3, periodic boundary conditions are used top and bottom for the displacement $\mathbf{u}$. The upper and lower variants entering from the right terminate in $\pi/2$ and 2ϕ walls, respectively; the deviatoric strain e_2 vanishes in the $\pi/2$ wall and the rotation $\omega_3 = \frac{1}{2}(u_{1,2}-u_{2,1})$ vanishes in the 2ϕ wall (both vanish in twin walls). Figures 3(b) and 3(c) give contour plots for e_2 and ω_3 in the fully relaxed state. On and outside the right edge, $\mathbf{u}$ was fixed at values for parallel twin walls normal to the edge and separated by $L/2$; the values of $\mathbf{u}$ (with zero average) were found by solution of the ordinary differential equation for e_2. The same solution was used on and outside the left edge, except that the walls are parallel to the edge; the latter lies at the center of a variant, with a twin wall at $L/4$ to its left. The system deals with the $\pi/2$ and 2ϕ walls very differently. It bends the twin walls away from the optimal 110-type walls to shorten the 2ϕ wall and to lengthen the $\pi/2$ wall, and then compensates for the latter by twisting the medium, in this way almost converting the $\pi/2$ wall to a twin wall of much lower energy.

This demonstration that the constrictions are 2ϕ walls agrees nicely with Refs. 17 and 18; note the high-resolution electron microscope pictures[17,18] and the moiré pattern.[18] But the broad ends are shown above to be $\pi/2$ walls deformed by rotation, not twin walls.[17,18] Observation of the difference would bolster the Landau theory ($|\Delta\omega_3|$ across a deformed $\pi/2$ wall would be about half that across a twin wall).

Similar narrowing in evolving structures is seen in Fig. 2 of Ref. 15 and Fig. 5 of Ref. 12, but that in Fig. 4 of Ref. 13 seems different (the deviatoric strain varies rapidly at the interface). The narrowing discussed above requires 2ϕ walls and so it is unrelated to the needle (lenticular) twins treated analytically in Ref. 3. The latter are seen in Fig. 2 of Ref. 3 and they appear also in some simulations;[12,13] they were not observed here, likely because of the fine scale of the figures.

E. Wall motion

Of course the conjugate-gradient process cannot describe properly most dynamical phenomena, but it should describe, qualitatively, slow processes like the wall motion below.

Figures 4(a)–4(c) show twin walls withdrawing from collision with orthogonal walls, rather than staying near the variant at the left (as in Fig. 3). The parameters and boundary conditions are as in the previous subsection, except that four walls enter, not two; the same results were found for $\mathbf{u}=0$ on and outside the left edge. The conjugate-gradient process was started with all four walls penetrating to one grid point from the left edge. After relaxing rapidly (over ≈ 600 conjugate-gradient steps) from this high-energy state, the energy then decreased almost linearly as the walls withdrew. At 1000 steps, with the walls still near the left edge, the variants have narrowed and broadened as in Fig. 3(b). At 3150 steps, the black variants (with $e_2<0$) have joined, separating the white variants; the narrow tips are now $\pi/2$ walls, and so they broaden as the twin walls withdraw. At 5000 steps, the tips of the white variants are again the wider. The later stages of the relaxation (lasting $\approx$ another 17000 steps) are uninteresting (they are severely affected by the right boundary conditions, which prevent complete withdrawal).

The main point is that the white tips are first narrow and later broad; in effect, twin walls change partners as they withdraw through an orthogonal wall. This process has not been noted in simulations. The narrowing-broadening effect should decrease with increasing distance from the orthogonal wall, as the inhomogeneous rotation has more room to operate. As described above, variants are observed[17,18] to narrow and broaden alternately on colliding with the orthogonal family. The exchange process explains why entry of an additional twin pair gives the same pattern, regardless of whether the pair enters a variant terminated by a $\pi/2$ wall or by a 2ϕ wall. Figures 4(d) and 4(e) show conjectured early and final stages in the penetration of two twin pairs (both terminating in twin walls); the other twin walls terminate some distance from the orthogonal wall at the bottom, forming either $\pi/2$ or 2ϕ walls. The left (right) pair collides with a $\pi/2$ (2ϕ) wall, adding a wall of each type; twin walls of the right pair switch partners, while those of the left do not. The process differs significantly from that shown in Fig. 1 of Ref. 3 (which did not discuss the 2ϕ and $\pi/2$ walls).

(a)

(b)

(c)
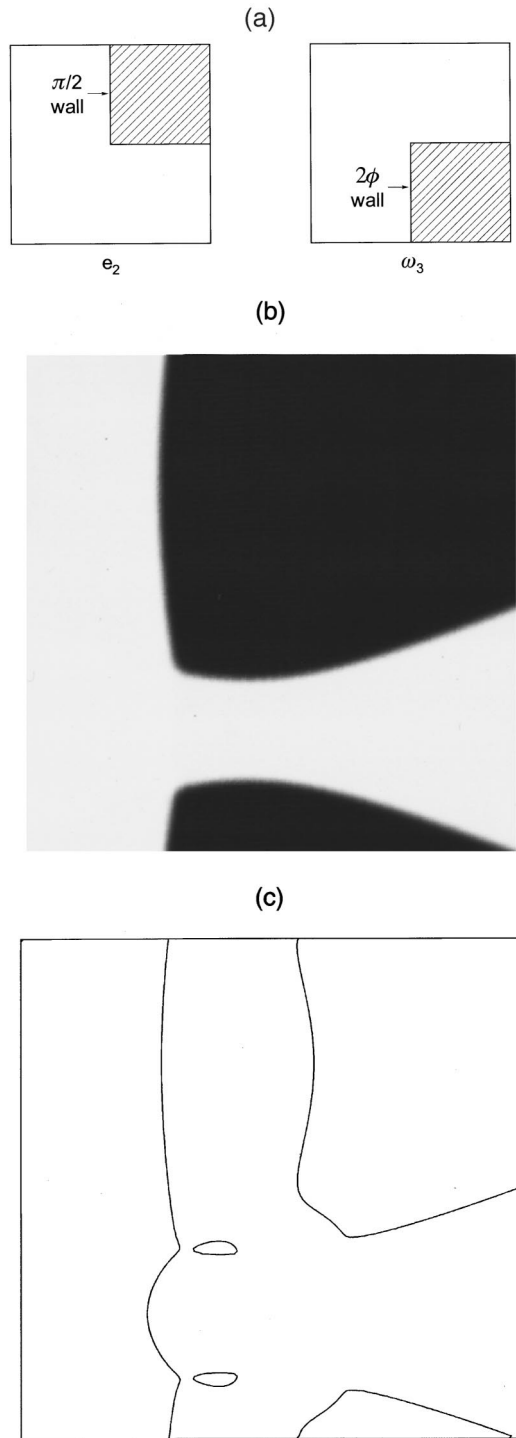

FIG. 3. Variant narrowing and broadening at the collison of a twin pair with the orthogonal family. The sides of the figures are parallel to T 110-type planes. Two twin walls impinge from the right onto a variant from the orthogonal set of otherwise identical walls, forming a 2ϕ wall and a $\pi/2$ wall which then relax. Part (a) shows the unrelaxed configuration; the deviatoric strain e_2 and the rotation ω_3 are positive (negative) in the unhatched (hatched) areas. Parts (b) and (c) give the fully relaxed configurations for e_2 and ω_3, respectively; the first is a grayscale contour plot, while the second gives the zero lines of ω_3 (the border is just a frame, not a zero line). The 2ϕ wall shortens, forming the constriction; the inhomogeneous rotation deforms the $\pi/2$ wall almost into a twin wall. The black $\rightarrow$ white range for e_2 is $-2.22\times10^{-3}\rightarrow+2.23\times10^{-3}$; ω_3 ranges from -3.73×10^{-3} to $+2.16\times10^{-3}$.

F. Tip splitting

Figure 5 shows the deviatoric strain for the lowest-energy state for twin walls colliding with a fixed boundary at 45°; the parameters are standard (Appendix B) except that $A_1 = A_6 = 50$. On and outside the right boundary, **u** is fixed at the solution for a chain of twin walls parallel to T 110-type planes; periodic boundary conditions are used top and bottom; the left boundary is fixed, with **u**=0 on and outside it. The interesting feature is that both tips split at the fixed boundary (this does not happen for $A_1 = A_6 = 10$). Two other states were found; only one tip splits in the intermediate-energy state, while both tips split very slightly in the highest-energy state. The interpretation is that tip splitting relieves stress locally without the large energy cost (linear in the size of the system) of introducing two more walls; the other side of the coin is that a tip, once split, likely nucleates penetration of the bulk by a pair of twin walls. Figures 8 and 11 of Ref. 12 also show tip splitting in comparable settings, but it seems only transiently, as part of the wall multiplication process. In contrast, the results described above show that the splitting occurs statically and also that it reduces the energy. The tip splitting observed[17,18] in electron microscopy of $YBa_2Cu_3O_{7-\delta}$ is different again; it appears at the collision of two twin families, in conjunction with the narrowing discussed above. The differences are not understood, but clearly the phrase ''tip splitting'' requires some caution.

G. Transformation front

The transformation likely proceeds by penetration of twinned product into parent material, thus avoiding a macroscopic displacement. Figure 6 shows the front, stabilized by a temperature gradient. The parameter values are as given in Appendix B, except that A_2 decreases linearly from left to right; the other boundary conditions are as for Fig. 5. The interface is parallel to 100-type walls; that is, one does not see the zigzag structure resulting from alternating T-O walls. Smaller gradients favor T-O walls, but then the structure is not so sharp; no zigzags were seen either for $1.5 \geq A_2 \geq 0.5$. A dynamical simulation[12] (with uniform T) found the same structure for the interface.

APPENDIX A: STRAIN-GRADIENT ENERGY

Equation (2.5b) for the gradient energy was used in Ref. 7; it is rotationally invariant (contrary to the statement in Ref. 24), but it omits three mixed terms of the same order:[24,8]

$$d_4(e_{1,1}e_{2,1}-e_{1,2}e_{2,2})+d_5(e_{1,1}e_{6,2}+e_{1,2}e_{6,1})$$
$$+d_6(e_{2,1}e_{6,2}-e_{2,2}e_{6,1}). \quad (A1)$$

The six coefficients d_1 to d_6 are independent (Ref. 24 disagrees). The d_5 and d_6 terms can, however, be omitted in leading order.[8] The coefficient d_4 is not measured experimentally, even its sign; this term performs no known impor-
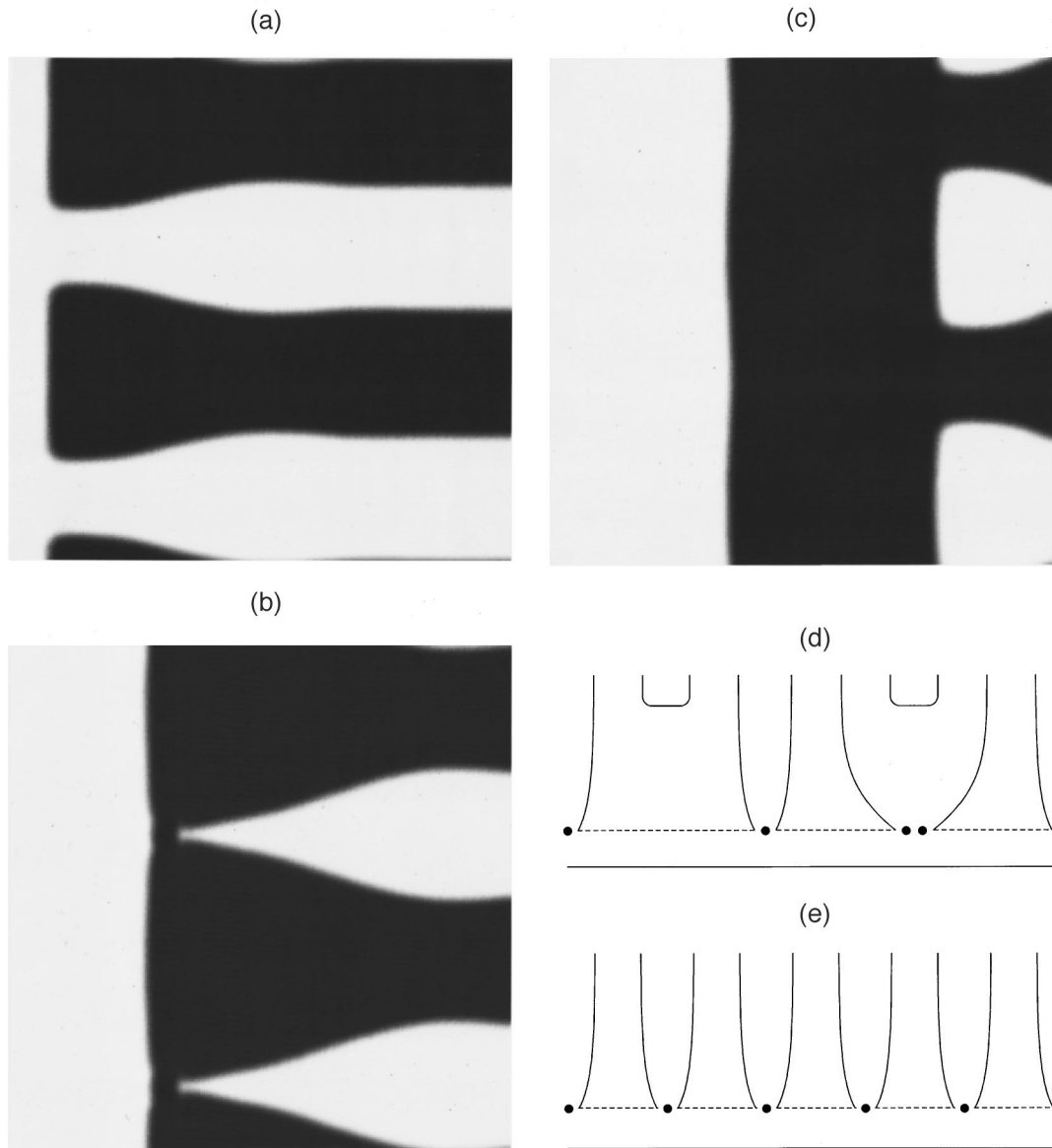
(a)

(c)

(b)

(d)

(e)

FIG. 4. Parts (a)–(c): Stages in the withdrawal of four twin walls from collision with the orthogonal family. Grayscale contours of the deviatoric strain e_2 are plotted after 1000, 3150, and 5000 conjugate-gradient steps. The walls change partners as they withdraw, the white tips first narrowing and then broadening. Parts (d) and (e): Conjectured early and final stages in the entry of two twin pairs. The solid lines are twin walls, the dashed lines $\pi/2$ walls, and the dots 2ϕ walls. The sides are parallel to T 110-type planes in all five parts.

tant role, it complicates matters, it even confuses issues, and so it should be omitted at this level.

The derivatives of ω_3 do not appear explicitly in the gradient part of the energy density because they are easily expressed in terms of the strain derivatives:[22]

$$\partial_2(e_1+e_2)=\sqrt{2}\,\partial_1(e_6+\omega_3)+\cdots, \tag{A2a}$$

$$\partial_1(e_1-e_2)=\sqrt{2}\,\partial_2(e_6-\omega_3)+\cdots, \tag{A2b}$$

where the dots represent higher-order terms; these relations, seldom discussed, arise from the same considerations as the compatibility relations. For example, the diagonal invariant $(\vec{\nabla}\omega_3)^2$ becomes

$$(\vec{\nabla}\omega_3)^2=-\frac{1}{2}(\vec{\nabla}e_1)^2+\frac{1}{2}(\vec{\nabla}e_2)^2+(\vec{\nabla}e_6)^2$$

$$+\text{ surface terms}+\cdots \tag{A3a}$$

with the help of Eqs. (A4) and (A6) of Ref. 8; a form for the surface terms is

$$\partial_1(u_{1,1}u_{2,12}-u_{1,22}u_{2,2})+\partial_2(u_{1,12}u_{2,2}-u_{1,1}u_{2,11}). \tag{A3b}$$

Equation (2.5b) can, it seems, be simplified further by keeping only the $(\vec{\nabla}e_2)^2$ term; the compatibility relation seems to provide sufficient coupling between the gradients. Reasonable results were found this way in unconstrained problems,[10,12] but constraints generate large dilatational and shear strains, and a separate investigation seemed necessary. Ten quenches were made for 100-type square grains and ten

FIG. 5. Tip splitting at the collision of twin walls with a fixed boundary at 45°. The figure gives a grayscale contour plot of the deviatoric strain e_2 for the ground state; the edges are parallel to T 100-type planes.

more for 110-type square grains, using the standard parameter set except that $d_1 = d_3 = 0$. No important differences were found; reasonably, the structures were more complex than with $d_1 = d_3 = 1$ (with more 90° bends), and the contours were more ragged (a finer grid would likely fix this).

APPENDIX B

The following collects details regarding the strain tensor, the Landau parameters, finite-strain theory, and the numerical procedure.
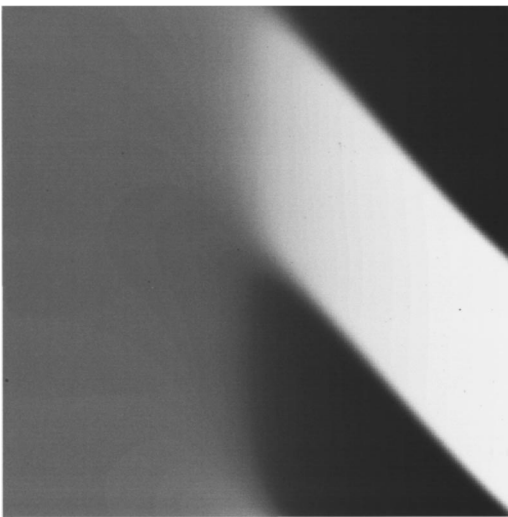

FIG. 6. Transformation front between tetragonal parent and twinned orthorhombic product. The figure gives a grayscale contour plot of the deviatoric strain e_2; the edges are parallel to T 100-type planes. The temperature decreases linearly from left ($A_2 = 52$) to right ($A_2 = -50$), with $T = T_c$ ($A_2 = 1$) midway between; the other boundary conditions are given in the text. The dilatational and shear strains are at most $0.3 e_{20}$ in magnitude.

1. Strain tensor and Landau parameters

For finite strains, the nonlinear term in the strain tensor is required so that a mere rotation of the space axes leaves the strain tensor, the strains, and the energy unchanged. The next subsection shows that finite-strain effects are a murky matter, best avoided at present, and so I assume infinitesimal strains (a common approximation—they are usually less than 10^{-3}). The computational effort is much reduced if the strain tensor is linearized. In most Landau theories, three parameters can be set by scaling the energy, the coefficient of the derivative term, and the order parameter; of course the other parameters change also. For the strain energy, in contrast, the scaling of the order parameter is possible only if the strains are small and if the tensor is linearized.

The standard parameter set was chosen after some experimentation, partly to reduce the computational effort and to reveal details (such as wall structure). The values $B_2 = -4 \times 10^6$ and $C_2 = 3 \times 10^{12}$ were chosen so that the T-O transition occurs at $A_2 = 1$, and the deviatoric strain there is $e_{20} = 10^{-3}$, both quite arbitrary values. The choice $d_2 = 1$ sets the unit of length; I set $d_1 = d_3 = 1$ as well. The strain e_{20} is much larger than the value (10^{-3}) at T_c if A_2 is too negative, and the order parameter is too soft if $A_2 \approx -1$ [the O-O' wall thickness diverges at T_c (Refs. 26 and 7)]. The value $A_2 = -50$ (where $e_{20} = 2.19 \times 10^{-3}$) was used for the most part, so that the wall width was much smaller than a typical variant (though not as small as in experiment). Results at $A_2 = -10$ were not qualitatively different.

The dilatational and shear stiffnesses are A_1 and A_6 at all T. For $T > T_c$, where the deviatoric stiffness is A_2, Ref. 10 argues for A_1 and A_6 both $\gg A_2$ (deviatoric soft, others hard). For $T < T_c$, the deviatoric stiffness is $A_2' = A_2 + 3 B_2 e_{20}^2 + 5 C_2 e_{20}^4$; some values are $A_2' = 4$, 11, 22, 61, and 240 at $A_2 = 1^-$, 0, -2, -10, and -50, respectively. The values $A_1 = A_6 = 10$ (deviatoric hard, others soft) were used in most cases; structures were too fine at much larger values, and ill-defined at much smaller ones.

2. Finite-strain theory

In finite-strain theory, e_1 is no longer simply proportional to the true dilatational strain $e_0(\mathbf{x}) = \Delta(\mathbf{x}) - 1$; here $\Delta(\mathbf{x})$ is the local ratio of the final to initial volumes, the Jacobian of the tranformation $\mathbf{x}' = \mathbf{x} + \mathbf{u}$. In two dimensions, $\Delta(\mathbf{x}) = [(1 + \sqrt{2} e_1)^2 - 2 e_2^2 - 4 e_6^2]^{1/2}$. Then, even though $e_1 = 0$, the volume decreases (by an amount of order e_2^2), even for the homogeneous state (and of course also for the O-O' wall and a periodic array of walls). Correspondingly, the displacement[25,8] acquires a term proportional to $(x_1 \pm x_2)\langle 1 - \Delta \rangle$. This term can be eliminated (or at least markedly reduced) by using the extended Landau theory of Ref. 8 and adjusting the coefficient of the additional term $E e_1 e_2^2$ so that no volume change occurs in the O state, or even a volume increase as usually observed. But then $e_1 \neq 0$, and so other linear terms are generated, corresponding to an overall shear, as seen from Eqs. (6.2) and (6.5) of Ref. 8. It seems inescapable that periodic boundary conditions, the natural choice to describe a chain of O-O' solitons, generate dilatational and shear strains once one deals with finite strains. These complications seem not worth facing for some time.

3. Numerical determination of the displacement field

Solution of the Euler-Lagrange equations (two fourth-order partial differential equations for the components u_i) was not attempted. Rather, the energy was minimized with respect to the components u_i. A grid of 201×201 points was set up (usually); the grid spacing was usually 0.1, giving a square of side length $L = 20$. The strains and their derivatives were expressed in terms of the displacement by means of centered, fourth-order, finite-difference approximations,[27] thereby trivially satisfying the compatibility equation (2.6). Application of the boundary conditions then gave the energy as a function of the components u_i at the grid points. The minimization, done by a conjugate-gradient method, was continued until numerical errors prevented further reduction of the energy; the number of iterations required was usually much fewer than the $\approx 8 \times 10^4$ independent variables. The displacement components for random starting states were chosen from a uniform distribution ($[-U, U)$, usually with $U = 10^{-3}$); the root-mean-square gradient $\delta F/\delta u_i$ of the energy decreased by typically 10 orders of magnitude from start to convergence.

In most Landau theories, the boundary conditions are applied to the order parameter; the analogy breaks down here as well: for ferroelastics they must be applied to the displacement **u**, not to the strains. The proper boundary conditions are obvious for grains ($\mathbf{u} = 0$ on and outside the boundary); but they may not be so obvious for other physical settings, and it may not be so easy to devise low-energy starting configurations.

References 12,13 use a very different procedure, expressing the energy solely in terms of e_2, though at the expense of introducing a nonlocal interaction; the oscillatory, anisotropic and long-range nature of the interaction[10,12,13] likely explains qualitatively the bending, bowing, and wobbling of the walls and also the narrowing and broadening found here, though the interaction needs modification to account for the constraints.

---

*Electronic address: jacobs@physics.utoronto.ca

[1] K. Aizu, J. Phys. Soc. Jpn. **27**, 387 (1969).

[2] E. K. H. Salje, *Phase Transitions in Ferroelastic and Co-elastic Crystals* (Cambridge University Press, Cambridge, 1993).

[3] E.K.H. Salje and Y. Ishibashi, J. Phys.: Condens. Matter **8**, 8477 (1996). A comprehensive discussion of needle twins is given by E.K.H. Salje, A. Buckley, G. Van Tendeloo, Y. Ishibashi, and G.L. Nord, Jr., Am. Mineral. **83**, 811 (1998).

[4] F. Falk, Z. Phys. B: Condens. Matter **51**, 177 (1983).

[5] G.R. Barsch and J.A. Krumhansl, Phys. Rev. Lett. **53**, 1069 (1984).

[6] J. Sapriel, Phys. Rev. B **12**, 5128 (1975).

[7] A.E. Jacobs, Phys. Rev. B **31**, 5984 (1985).

[8] A.E. Jacobs, Phys. Rev. B **46**, 8080 (1992).

[9] S. Kartha, T. Castán, J.A. Krumhansl, and J.P. Sethna, Phys. Rev. Lett. **67**, 3630 (1991).

[10] S. Kartha, J.A. Krumhansl, J.P. Sethna, and L.K. Wickham, Phys. Rev. B **52**, 803 (1995).

[11] A.E. Jacobs, Phys. Rev. B **52**, 6327 (1995).

[12] W.C. Kerr, M.G. Killough, A. Saxena, P.J. Swart, and A.R. Bishop, Phase Transit. **69**, 247 (1999).

[13] S.R. Shenoy, T. Lookman, A. Saxena, and A.R. Bishop, Phys. Rev. B **60**, 12 537 (1999).

[14] S. Semenovskaya, Y. Zhu, M. Suenaga, and A.G. Khachaturyan, Phys. Rev. B **47**, 12 182 (1993), and references therein.

[15] A.M. Bratkovsky, E.K.H. Salje, and V. Heine, Phase Transit. **52**, 77 (1994), and references therein.

[16] P. Klouček and M. Luskin, Continuum Mech. Thermodyn. **6**, 209 (1994); Math. Comput. Modell. **20**, 101 (1994); B. Li and M. Luskin, Mater. Sci. Eng. A **273**, 237 (1999).

[17] A.H. King and Y. Zhu, Philos. Mag. A **67**, 1037 (1993).

[18] Y. Zhu, M. Suenaga, and J. Tafto, Philos. Mag. A **67**, 1057 (1993).

[19] References 9 and 10 also found a complex energy surface, but for completely unrelated reasons; the density in Refs. 9,10 contains explicit bulk inhomogeneities.

[20] A convenient reference is L. Brillouin, *Tensors in Mechanics and Elasticity* (Academic, New York, 1964).

[21] The parameters a and T_0 could, in principle, be fitted from the transition temperature T_c and the stability limits; the T state is unstable for $A_2 < 0$, and the O state is unstable for $A_2 > B_2^2/(4C_2)$.

[22] S.F. Borg, *Matrix-Tensor Methods in Continuum Mechanics* (Van Nostrand, New York, 1963). This gives a particularly thoughtful derivation of Eqs. (2.6) and (A2), both the linearized versions and the leading nonlinear corrections.

[23] The compatibility relation for finite strains is given, for example, by W. Jaunzemis, *Continuum Mechanics* (MacMillan, New York, 1967), Eq. (15.20).

[24] G.R. Barsch and J.A. Krumhansl, Metall. Trans. A **19**, 761 (1988).

[25] J.L. Ericksen, Int. J. Solids Struct. **22**, 951 (1986).

[26] J. Lajzerowicz, Ferroelectrics **35**, 219 (1981).

[27] Centering the derivatives causes the strains to extend two grid points into a region where the displacement vanishes identically.